CFD for engineers

Einar Aasli [5149819] - Morgane Bourgeois [5159822]

November 15^{th}, 2019

Instructor: Prof. Stefan Hickel
Faculty: Aerospace Engineering

Abstract

Computational Fluid Dynamics is used to perform simulations which can not be done experimentally or to be able to extract all quantities required in a defined domain without introducing any measuring instruments that would disrupt the flow field. Because of the computing cost, the real-time simulations of the governing equations are restricted. That is why several numerical method were developed through years to resolve the governing equations have been leading to decrease computational cost. Since it is about numerical approximations the accuracy of a simulation may vary from one method to another according to the grid refinement, the time scheme or the turbulence model used. This report presents a discussion on these different aspects.

Contents

1 Introduction

This report compares different resolution models for computational fluid dynamics based on the 2D steady state simulations of a high loaded transonic turbine nozzle guide vane, so-called VKI S1 Nozzle.

The problem being 2D the RANS method is used and studied here. The RANS method resolve the Navier-Stokes equations by decomposing the vector field into mean values and fluctuations. This decomposition leads to the Navier-Stokes equations for the average which include the Reynolds stress tensor. Several turbulent model provide approximations for the Reynolds stress tensor.
The influence of the grid refinement, the choice of the time scheme and the turbulence model are discussed in this report.

2 Grid generation

2.1 Computational domain

The first step to generate a grid around the blade is to set the computational domain. After creating the blade geometry with the given blade coordinates, a suitable computational domain has been created. Because the upper and the lower domain boundaries are periodic, edges have to perfectly fit together. The inlet has been imposed to be at 55mm upstream of the blade's leading edge. The outflow boundary should be far enough from the blade to limit unphysical effects.

Taking into account all these information and to make sure to get the most suitable computational domain a Python script which returned edge profile of the blade between the maximum ordinate and abscissa as shown in figure 1 has been used. Still by using the Pyhton script, from this portion of curve, the rest of the upper boundary has been generated. The lower boundary has simply been created by reproducing the upper one 57.5 mm below. Straight lines stretching in the same direction as the end of python generated curves continues the upper an lower part of the computational domain down to the outlet. In order to avoid unnecessary curvature of the boundary lines, the outlet was set as a straight line connecting the lower and upper part of the boundary and is hence parallel to the inlet. This would make the blocking and and meshing easier since it did not require to mesh a curled outlet region. The 2 shows the entire computational domain.

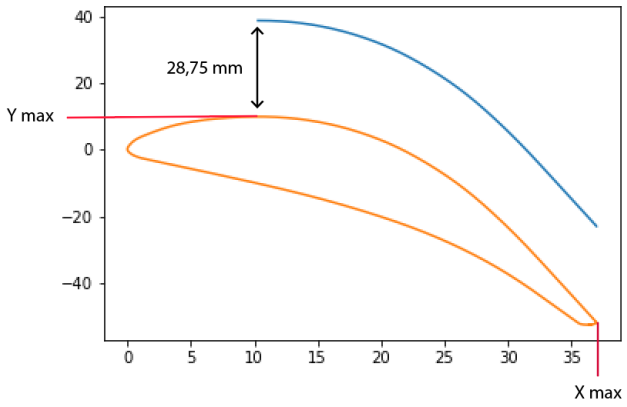

Figure 1: Portion of the blade generated via a Python script

2.2 Blocking

Second step to generate a grid around the blade is to create blocks in order to conceive the mesh from the blocks' edges. The geometry of each blocks provide the direction of the mesh lines. Hence it is really important to make sure that the chosen geometry leads to non overlapping nodes, positive cell volume and orthogonality of the mesh according to the flow direction. Also, the location of the vertices of the blocks is determinant in the smoothness of the grid.

The most suitable grid for this problem is the O-grid around the blade. The domain is decomposed in two levels. The sub domain has been created in such a way that the mesh is as orthogonal as possible around the blade. The coarse level has been made such that the grid lines are aligned with the streamlines. All these precautions are important for a structured grid in order to reduce the effect of numerical diffusion. Because the problem is periodic between the upper and lower boundaries the grid lines have to be as orthogonal as possible with these boundaries. The blocking is shown in figure 3.

2.3 Coarse grid (grid 1)

The figure 4 shows the coarse grid which is made of 20047 cells. Exponential stretching rule has been used all along the blade, in the sub-domain in the orthogonal direction of it, as it can be seen in figure 5. It has also been used parallel to

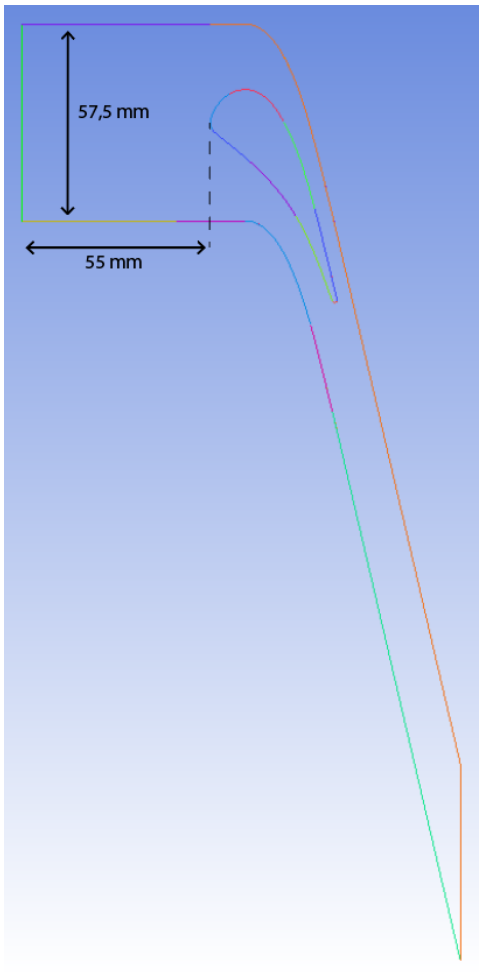

Figure 2: Computational domain

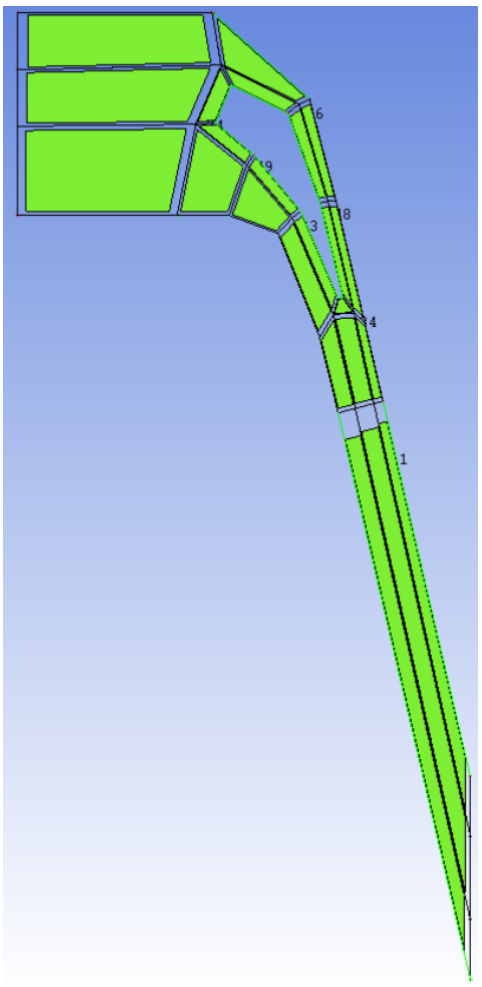

Figure 3: Blocking

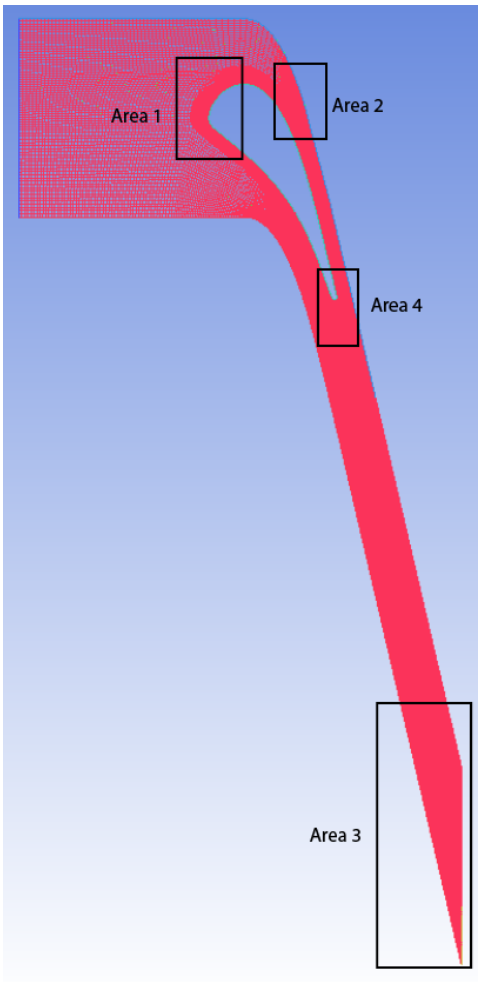

Figure 4: Coarse grid

the blade to smooth the grid near the wake. Everywhere else stretching rule used has been the uniform one.

Because of the periodicity condition for the upper and lower boundaries, meshes must be as orthogonal as possible with each other. We can see that in figure 6 that it is the case for this mesh. Also, there is not hole between the two boundaries so the periodicity condition has been respected.

At a more detailed level several values need to be check to evaluate the quality of the mesh : cells volume should be positive, the determinant greater than 0 en the minimum angle greater than 30°. The mesh presented here have the following information :
- Minimum quality for "Volume" : 0.0116 m^2
- Minimum quality for "Determinant" : 0.866
- Minimum quality for "Min angle" : 12.6°

Just by looking at the mesh the smoothness of it can be evaluated. By zooming on the area 1 of the figure 4 which is shown in figure 5, we can see that the smoothness of the grid could be improved by rearranging the location of the vertices of the blocks a bit better. There is a significant volume change from the cells in the inlet region to those in the O-grid layer near the leading edge of the blade, and there is a quite sharp angle linked to the vertex in the middle of the picture. One way to improve the volume transition would be to decrease the number of nodes outwards from the O-block. But as can be seen from figure 6 this would make the volume change bigger in this smoother area. Because all the blocks are connected, making the mesh smoother in one given area can lead to badly change it in an other one. After compromising, the grid was kept the way it looks. The best way to fix this would be to place the vertex more towards the inlet, making a greater angle and a smoother transition. Considering that the angles of the mesh in this area was over the benchmark of 30°, we assume that it is smooth enough to run a viable simulation on it.

The volume and determinant criteria are respected while the minimum angle of this mesh is too low. The figure 7 shows the location of angles below 30°. These bad angles came from the initial geometry of the computational domain. The way in which the domain has been geometrically stopped automatically results in too sharp angles at the outlet boundary. The angle between the outlet and the lower boundary is already smaller than 30°. The mesh being orthogonal to the boundaries many sharp angles are located in this area. A way to solve this problem would have been to create the outlet

with an angle of 90° with the upper and the lower boundaries as shown by the red line in figure 7, but this would interfere with the periodic boundary condition and hence not be a solution for this flow problem. In retrospect, a curvature from the linear region to the outlet would be the best option, but more advanced blocking could, if not properly done, have more angles less than 30°. Hence, assuming this part to be far enough from the blade to not disrupt the simulation too much, this was maybe a good solution after all.

Another weakness of the mesh is, as can be seen in figure 8, the volume change in the wake region. In order to obtain a smooth mesh near the trailing edge, the mid-block further away from the wake became to wide. This should have been improved by making the block narrower in the far wake region.

In the region following the sides of the blade and near the trailing edge, the mesh is very smooth and of good quality, as can be seen from figure 5. The exponential stretching of nodes along the blade in the O-grid is also of decent quality. So despite its worse areas, the grid is of some quality in important regions.

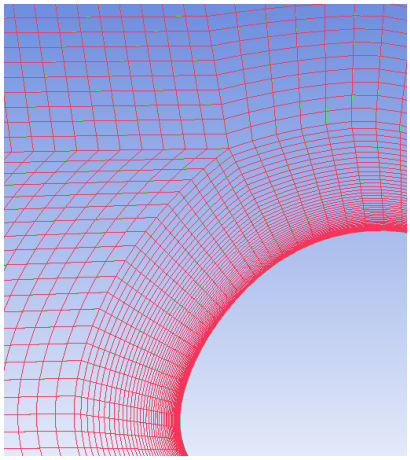

Figure 5: Zoom on area 1 shown in figure 4

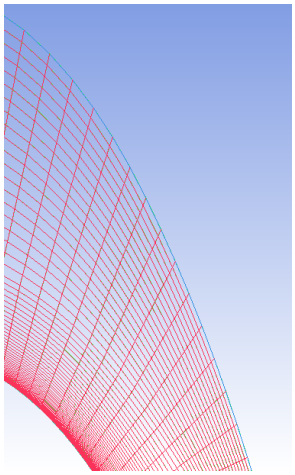

Figure 6: Zoom on area 2 shown in figure 4

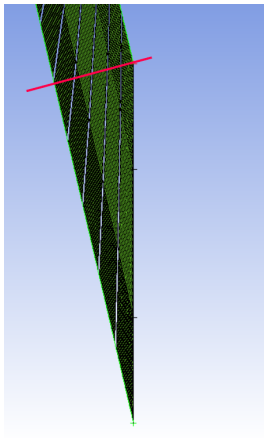

Figure 7: Zoom on area 3 shown in figure 4

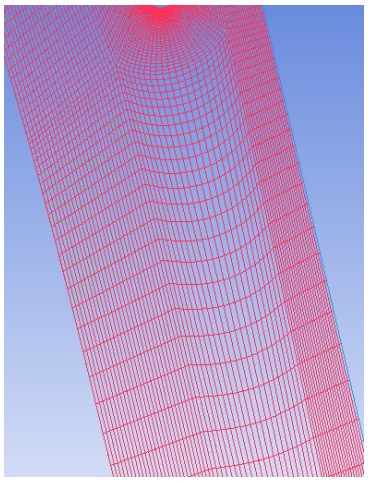

Figure 8: Zoom on area 4 shown in figure 4

2.4 Fine grid (grid 2)

The refinement of the coarse grid is guided by the values of Y+ along the blade which is the non-dimensional wall distance for a wall-bounded flow. The figure 9 shows the Y+ values for the coarse grid. Its maximum value is above 10. To be able to compare the effects of the spatial discretization on the convergence of the simulation and on the results this coarse grid is refined. A good refinement of this grid would provide a Y+<1 making sure that it is not too low either. The figure 10 shows the Y+ values for the fine grid.

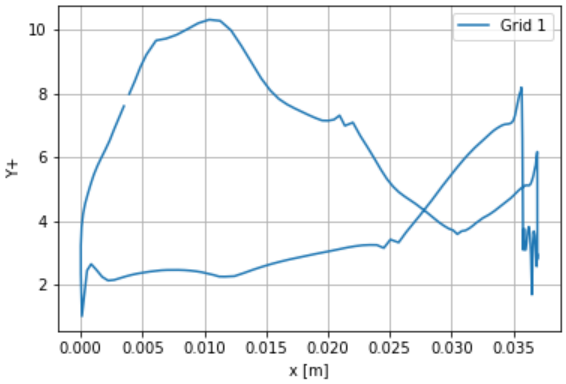

Figure 9: Y+ for the coarse grid

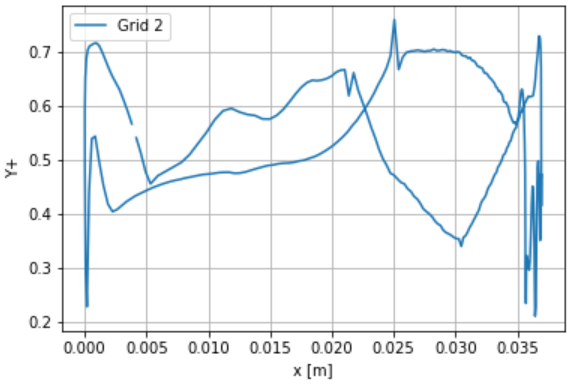

Figure 10: Y+ for the fine grid

The refined mesh, which is composed of 33250 cells, have the following information :
- Minimum quality for "Volume" : 0.000658 m^2
- Minimum quality for "Determinant" : 0.897
- Minimum quality for "Min angle" : 12.4°

The minimum angle is still too low but these angles are located in the same area as explained for the coarse mesh and could be done little with. Except for near the outflow, the mesh is still within the limits of orthogonality. Y+ is less than 1 all along the blade, which make the fine grid satisfy the design criteria. These Y+ plus values were achieved by placing the first node normal to the blade closer to the blade boundary. More cells were been added making the grid finer and in some areas better than the coarse one. However one should notice that the amount of nodes outward from the blade in the O-grid has not increased, while the amount in tangential has. The coarse grid is maybe too fine in the O-grid, but the amount of cells in the fine grid is more appropriate. Some blocks on the right side of the blade have been made narrower and some vertices near the trailing edge have been moved to improve the wake, as can be seen from figure 11 and figure 15. Area 1 seen in figure 13 have gotten a smoother transition from O-grid to H-grid due to the movement slight movement of the vertex in the middle, more cells outside the O-grid and a first cell closer to the blade. Still, there is quite a sharp angle at the vertex in the middle. As discussed above for the coarse grid, the improvement in this area have made area 2 worse with a bigger volume change (see figure 14). Still, the area along the airfoil is good and the refinement in far wake has improved its overall smoothness.

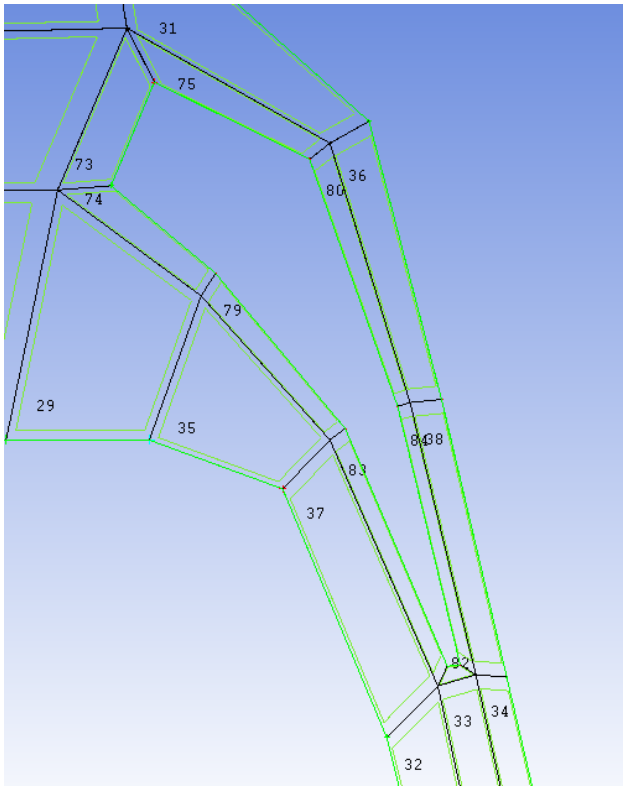

Figure 11: Blocking for the fine mesh

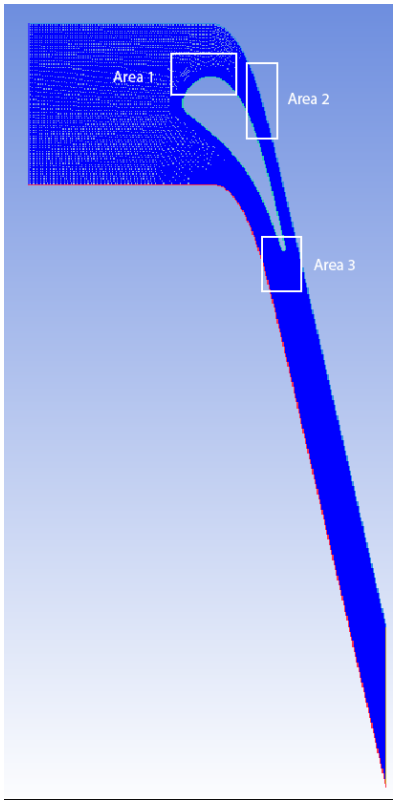

Figure 12: Fine grid

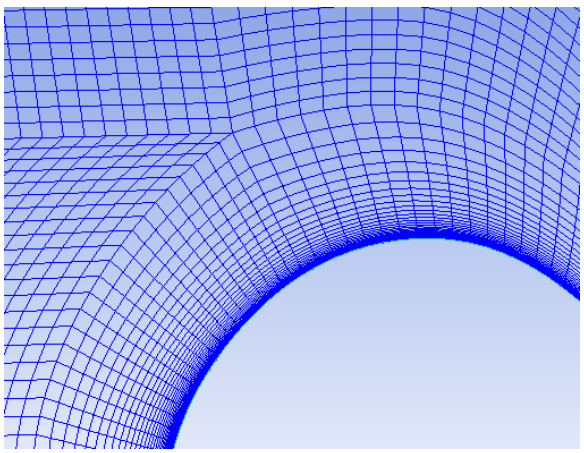

Figure 13: Zoom on area 1 shown in figure 12

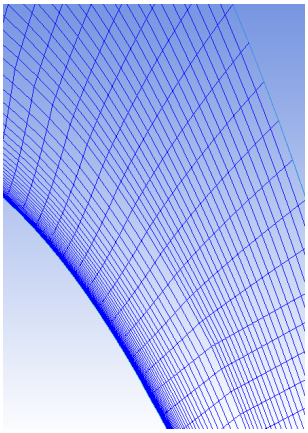

Figure 14: Zoom on area 2 shown in figure 12

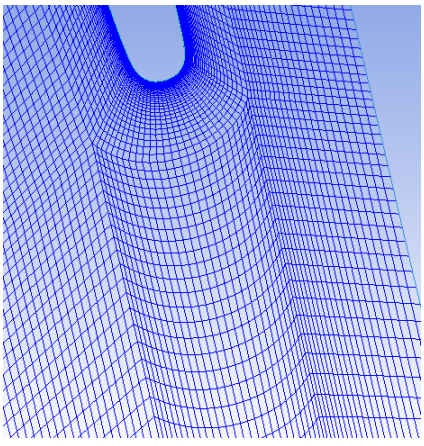

Figure 15: Zoom on area 3 shown in figure 12

3 Initial and boundary conditions

The flow is considered to be a compressible flow of air considered as an ideal gas with a dynamic viscosity given by Sutherland's law [3] :

$$\mu = \mu_{ref} \left(\frac{T}{T_{ref}} \right)^{3/2} \frac{T_{ref} + S}{T + S} \tag{1}$$

With the following coefficients for the air : $T_{ref} = 273.15$ K, $\mu_{ref} = 1.716 \cdot 10^{-5}\ kg \cdot m^{-1} \cdot s^{-1}$, $S = 110.4$ K.

The inflow is subsonic and normal to the inlet. To be able to impose the total energy and the total pressure at the inlet boundary a total energy for the heat transfer fluid model has been chosen. So, as boundary conditions for the inlet the total pressure has been set at 90400 PA and the total temperature at 409K . As requested the k-omega SST turbulence model and a turbulence intensity of 3% with an automatic length scale have been defined .

The outflow is normal to the outlet. The static pressure has been set at 52295 Pa at this boundary. The blade is considered as a wall at 300K. The upper and lower boundaries are periodic. The 'high-resolution' scheme for the spatial discretization has been used. For the time-stepping scheme the 'Auto Timescale' for the timescale control has been chosen. In using that option CFX determines time step automatically based on the boundary conditions, flow conditions, physics, and domain geometry, which are parameters that have been clearly defined.

4 2D steady state simulation

The aim of the simulation is to evaluate the influence on results of the spatial discretization, the time discretization and the turbulence model. In the following table results for each configuration are sum up :

Table 1: Results for different configurations

Grid	Turbulent model	Time scheme	Drag force [N]	Lift force [N]
1	k-ω SST	'high resolution'	20.3576	8.61624
2	k-ω SST	'high resolution'	20.3725	8.60175
1	k-ω SST	upwind scheme	20.3805	8.30649
2	k-ω SST	upwind scheme	20.3903	8.35388
2	BSL EARSM	'high resolution'	20.3731	8.60679

4.1 Result interpretation

In this section the results are interpreted for the simulation on the coarse grid with an 'high-resolution' time scheme and a k-ω SST model for the turbulence. From the residual plots in figure 16 one can observe convergence. The simulation was run for a few hundred more iterations after convergence in order to let the slower converging error converge. From all the contour plots the periodic boundary condition seem to work with continuous flow properties across the boundaries. From figure 18 we can see that the Mach number at the inlet is almost zero. The Mach number near the outlet is around 0.83. As expected, there is a high pressure region beneath the blade and a strong acceleration with lower pressure and higher mach number on the upper side of the blade. Where the temperature decreases on the top side of the blades and downstream, the Mach number increase. According to the definition of the Mach number $Ma = \frac{U}{\sqrt{\gamma RT}}$ this behaviour is physical. As stated in the problem description, the flow should be transonic which validates a Mach number over 1 in certain regions. On the right side of the blade a flow separation can be observed with a discontinuity in flow velocity as one would expect from a highly loaded airfoil.

The pressure just outside trailing edge is low, as one would expect with a higher Mach number than on the bottom side of the blade. At the same time, the Mach number just to the left of the trailing edge changes rapidly from around 1 and almost to 0. From 24 (blue line) one can observe some strange crossing in the plot of the pressure coefficient for the the trailing edge. It is not clear if this behaviour is physical, but the characterises of a shock with drastic drop in Mach number over 1 is occurring and may be a possible explanation. However this shock behavior does not seem to continue down to the suction side of the blade beneath, even though the Mach number here is higher than 1 too. Maybe this area was not resolved with a fine enough grid to capture shock all the way down to the suction side.

When it comes to boundary layer resolution, the Y+ values around the blade range from around 1 to around 11 as can be seen in figure 9. To resolve the boundary layer around the airfoil, Y+ should be placed in the viscous sub layer at a Y+< 5 or ideally Y+< 1, so the grid is too coarse. However CFX uses automatic wall functions to model the boundary layer and give more accurate results. But the coarse grid may be to fine for these wall functions since the models usually are not valid if the first cell is placed in the log-law layer with 30 <Y+< 300 (ideally a bit over 30). If one zooms in on the boundary layer on the bottom side of the airfoils, some oscillating behaviour in Mach number is seen along the blade.

This may be a consequence of the badly modeled or resolved boundary layer. Hence, the simulation got a clear source of error that may be corrected with a y+< 1.

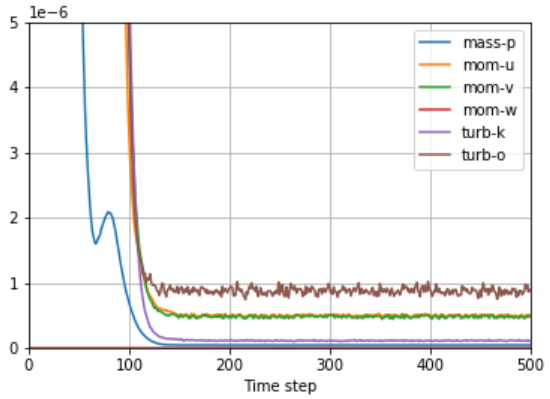

Figure 16: Residuals [configuration : line 1 of the table 1]

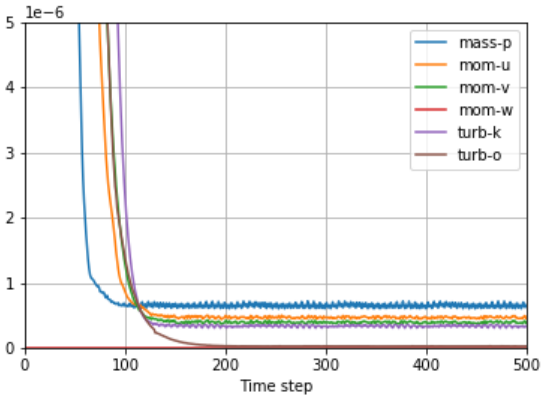

Figure 17: Residuals [configuration : line 2 of the table 1]

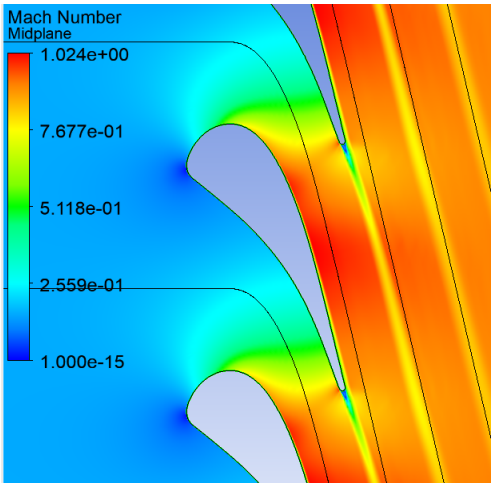

Figure 18: Mach number [configuration : line 1 of the table 1]

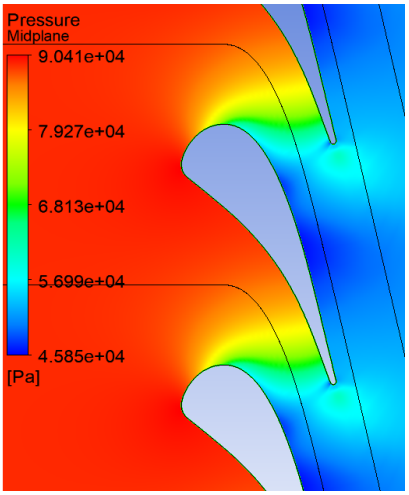

Figure 19: Static pressure [configuration : line 1 of the table 1]

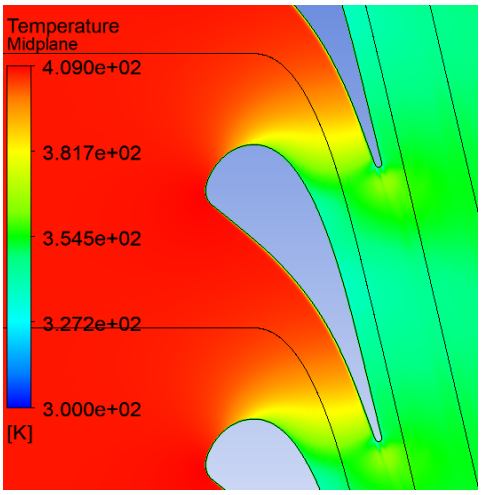

Figure 20: Temperature [configuration : line 1 of the table 1]

4.2 Evaluation of the grid refinement

The coarse grid and the fine grid are compared for a resolution with an 'high-resolution' time scheme and a k-ω SST turbulent model.

The figure 16 and the figure 17 show that the simulation converged for both grids. That means that the simulation has reached an equilibrium state, hence the data can be analyzed. Both simulations reach the convergence after approximately the same number of iteration, but because the fine grid includes more cells than the coarse one the computing time per iteration for the grid 2 is higher.

The values of the Mach number (fig. 18 and fig. 21) and of the pressure (fig. 19 and fig. 22) are little higher for the fine grid than for the coarse grid. The values for the temperature don't seem to be affected by the refinement of the grid (fig.20 and fig. 23). However the results are very close, the difference between these values is of order 10^{-3}. Overall these two simulations are comparable.

Interestingly, the boundary layer around the blade looks quite similar to the coarse grid. The Y+ values are all beneath one and should have enough resolution to simulate the viscous boundary layer. These similarities verifies the coarse grid and may be a result of CFX providing good wall functions. The oscillating behaviour on the down side of the blade are no longer there, but does not seem to have effected the flow outside the boundary layer. Hence the wall functions provided in CFX may provide good enough model for the boundary layer.

When it comes to the high Mach number at the left side of the trailing edge, it is slightly lower but still occurs. There may still be lack of resolution, but since the results for the two grids are so similar it is hard to say.

Figure 24 shows the pressure coefficient all around the blade for both grid. This coefficient is similar for the fine and coarse grid at the the blade's leading edge. At the blade's trailing edge, the fine grid provides values of Cp that overlap less than for the coarse grid. We can conclude that the simulation in more accurate at the trailing edge for the fine grid.

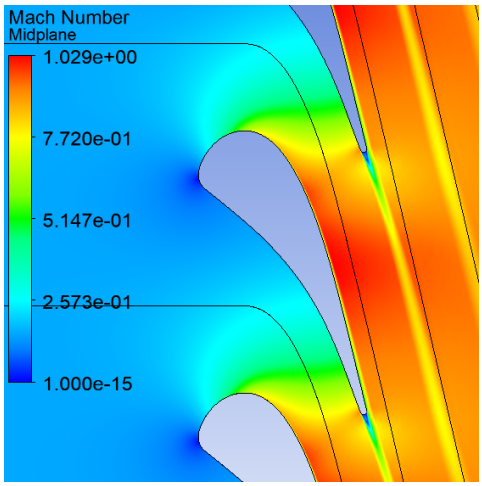

Figure 21: Mach number [configuration : line 2 of the table 1]

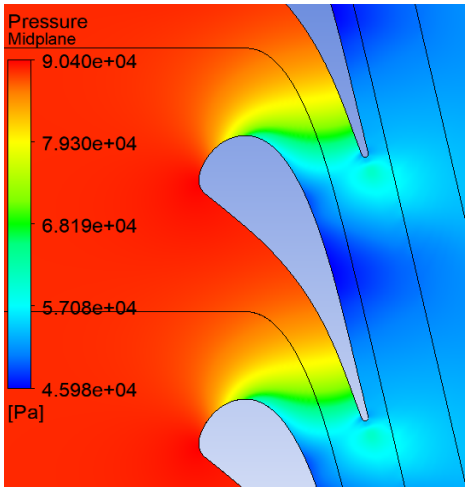

Figure 22: Static pressure [configuration : line 2 of the table 1]

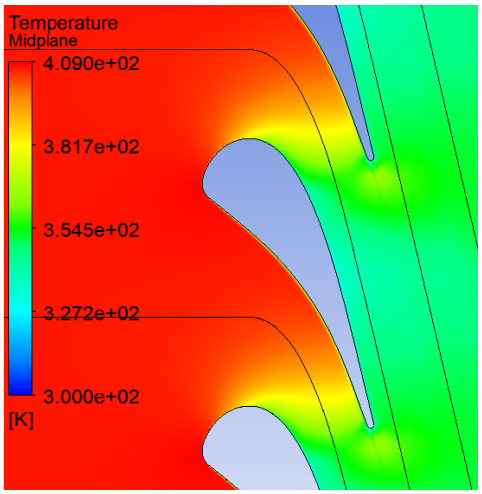

Figure 23: Temperature [configuration : line 2 of the table 1]

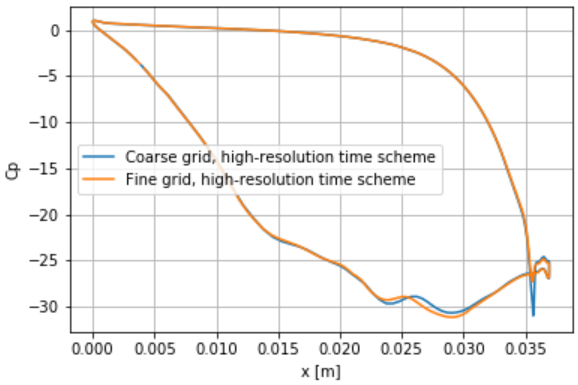

Figure 24: Pressure coefficient

4.3 Evaluation of the numerical diffusion

The influence of the time scheme is evaluated for both grids. In each case the 'high-resolution' scheme, which is a second order scheme, is compared with the upwind scheme, which is a first order scheme.

4.3.1 Coarse grid

The figure 25 confirms that the simulation converged for the upwind scheme. The number of iterations needed is comparable with the 'high-resolution' scheme (fig. 16), but the computational cost for each iteration is higher in the case of the high-resolution scheme.

The values of the Mach number is lower (fig. 27) whereas the values for the pressure is higher (fig. 28). Like for the evaluation of the grid refinement, the values of the temperature don't seem to be affected by the time scheme used (fig. 29). The values of the pressure coefficient all around the blade is more affected by the time scheme for the lower edge of the blade than for the upper one (fig. 26).

4.3.2 Fine grid

The figure 30 confirms that the simulation converged for the upwind scheme. Like for the coarse grid the number of iteration for the upwind scheme is similar to the 'high-resolution' one (fig. 17).

The values computed follow the trend already observed for the coarse grid, that is, lower values for the Mach number (fir. 32), higher ones for the pressure (fig. 33) and any noticeable change in the values of the temperature (fig.34). The values of the pressure coefficient all around the blade is more affected by the time scheme for the lower edge of the blade than for the upper one (fig. 31).

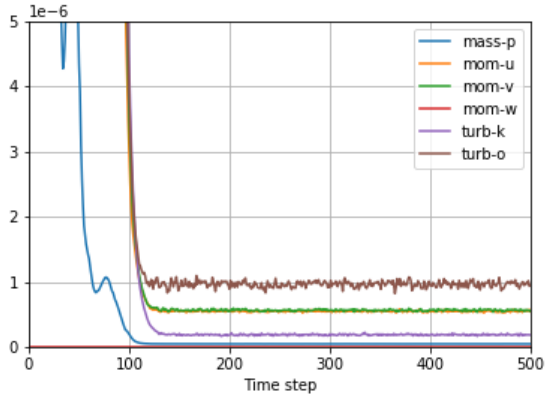

Figure 25: Residuals [configuration : line 3 of the table 1]

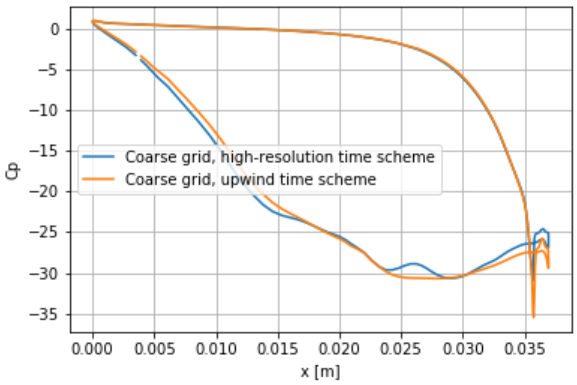

Figure 26: Pressure coefficient

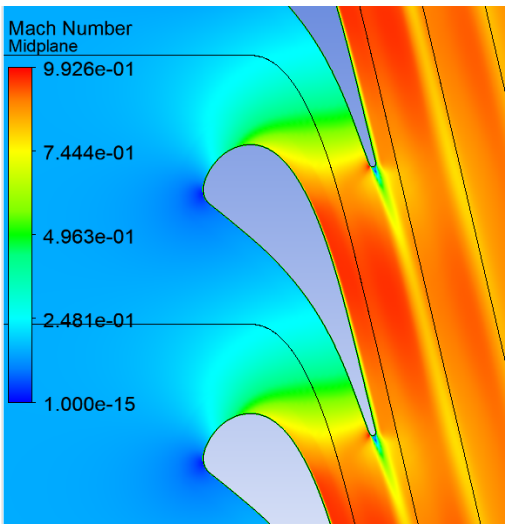

Figure 27: Mach number [configuration : line 3 of the table 1]

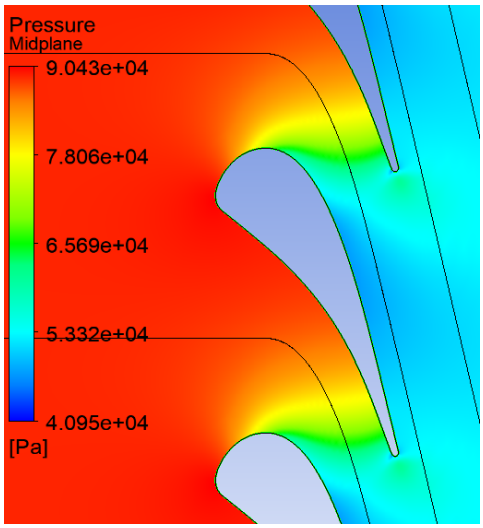

Figure 28: Static pressure [configuration : line 3 of the table 1]

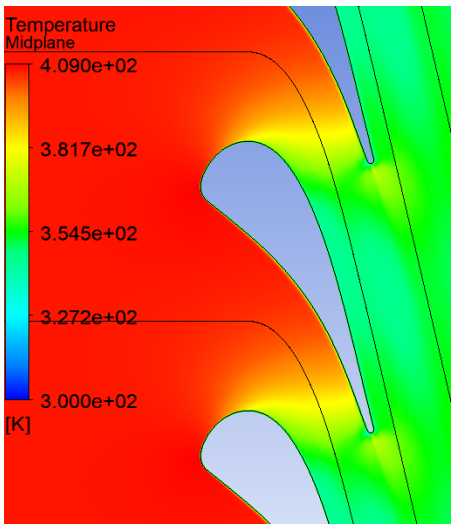

Figure 29: Temperature [configuration : line 3 of the table 1]

4.3.3 Comparison

The numerical diffusion depends, as the same time, of the order of the time scheme used and of the refinement of the grid. In general terms, a first order scheme should provide less numerical diffusion for a coarse grid than an second order scheme and vice versa. By comparing the values of the 4 cases studied until that point, we can notice that the choice of the time scheme have a greater influence on the results of the fine grid than of the coarse grid.

An high-resolution scheme requires more smoothness of the grid to work properly. The refinement of a mesh is valuable as a simulation on a fine grid is more accurate if it uses a high order time scheme. In that case the boundary conditions need to be well-initialized. In addition a fine mesh leads to a grid-independent solutions that prevent the effects of grid resolution on the numerical loss. B. van Leer in his study on Upwind and High-resolution methods for compressible flows [4] shows that the first-order upwind scheme could be useful for debugging or for studying the quality of the numerical flux near a sonic point. It can also be used to increase the user's confidence in the choice of boundary conditions before proceeding with the simulation with a 'high-resolution' scheme.

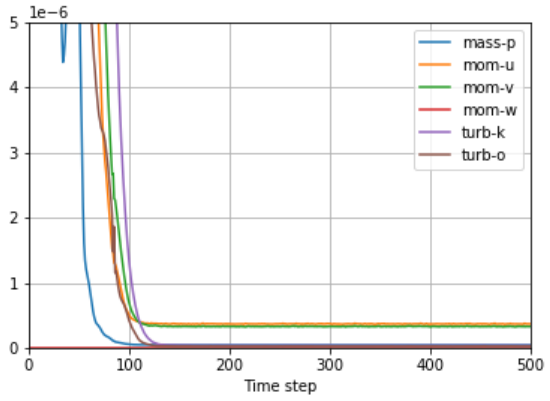

Figure 30: Residuals [configuration : line 4 of the table 1]

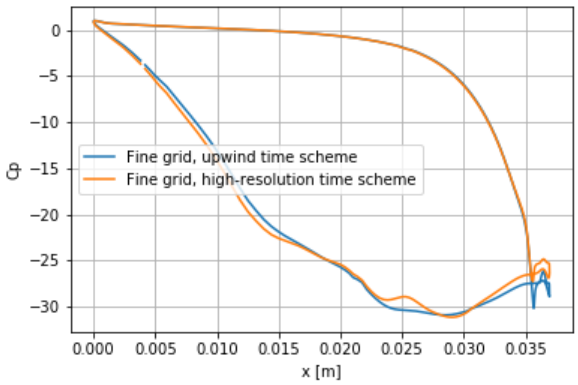

Figure 31: Pressure coefficient

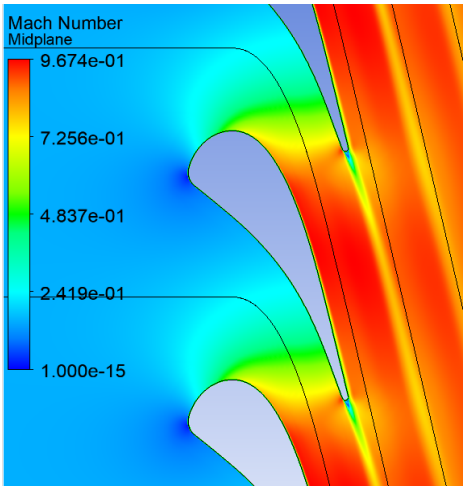

Figure 32: Mach number [configuration : line 4 of the table 1]

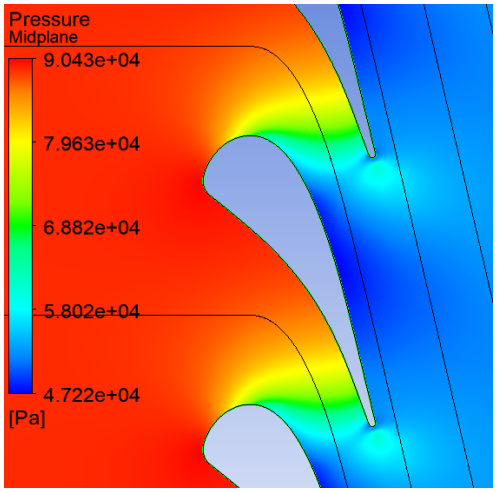

Figure 33: Static pressure [configuration : line 4 of the table 1]

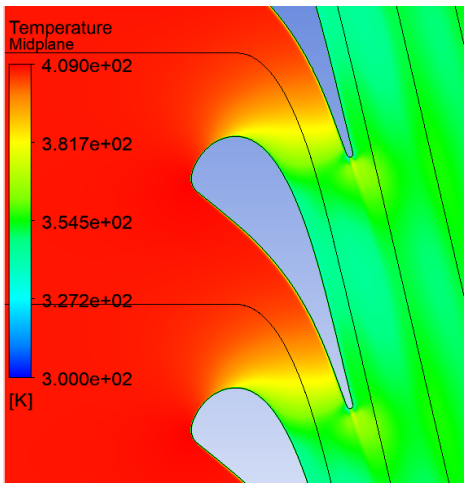

Figure 34: Temperature [configuration : line 4 of the table 1]

4.4 Evaluation of the turbulent model

A turbulence model that can better account for anisotropic turbulence is the EARSM (Explicit Algebraic Reynolds Stress Models) with the ω-equation-based Baseline (BSL) model. The Reynolds stress models (RSM) are higher level turbulence closures and give superior results for flows with anisotropic turbulence, but the convergence is slow and sometimes even not stable. By reducing the number of transport equations from reconstructing the Reynolds stress tensor or anisotropic eddy viscosity tensor the EARSM are much less demanding than RSM from the computational standpoint and, at the same time, are capable of reproducing some important features of turbulence as anisotropy [2].

The figure 35 confirms that the simulation converged for the BSL EARSM model.

The problem being anisotropic at the blade this turbulent model is more accurate for this study than the k-ω SST model. However, the values of the Mach number (fig. 37), of the pressure (fig. 38) and of the temperature (fig. 39) are closer to the results obtain from the case 1 of the table 1. So it would seem that the use of a k-ω SST model is reasonably reliable for a simulation on a coarse grid. Furthermore, the pressure coefficient all around the blade is almost the same for both turbulent models (fig. 36). Hence both of the turbulent models provide accurate solutions for the blade studied here under the initial and boundary conditions described in the section 3.

5 Final remarks and conclusion

The most important concern of Computational Fluid Dynamics is to provide the most accurate results with a reasonable computational cost. Several elements, that influence this cost, are to be taken into consideration : the grid refinement, the choice of the time scheme and the choice of the turbulence model. These latter are determined according to the study conducted.

All over, the results from the five simulated cases are very similar. There is hardly any difference between the refined

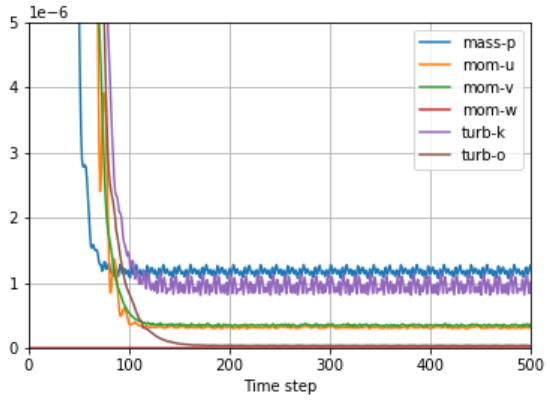

Figure 35: Residuals [configuration : line 5 of the table 1]

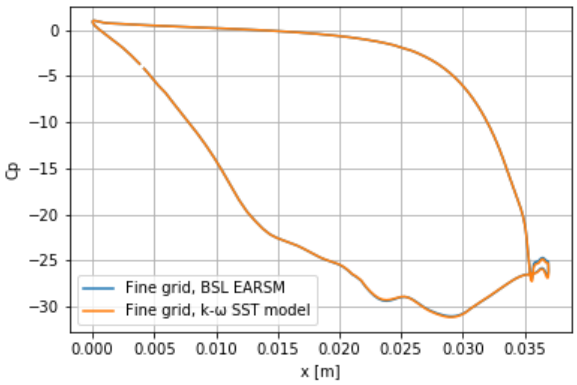

Figure 36: Pressure coefficient

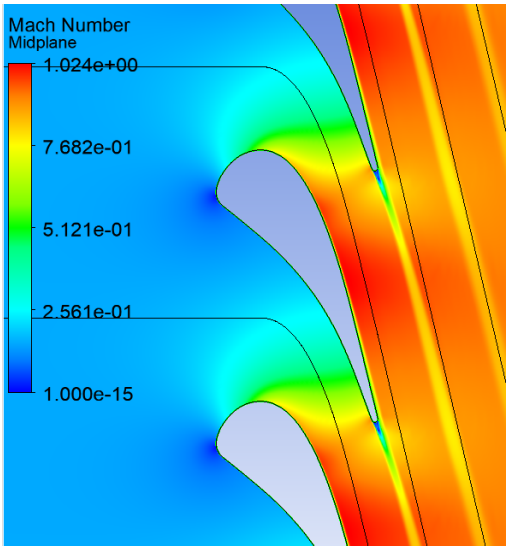

Figure 37: Mach number [configuration : line 5 of the table 1]

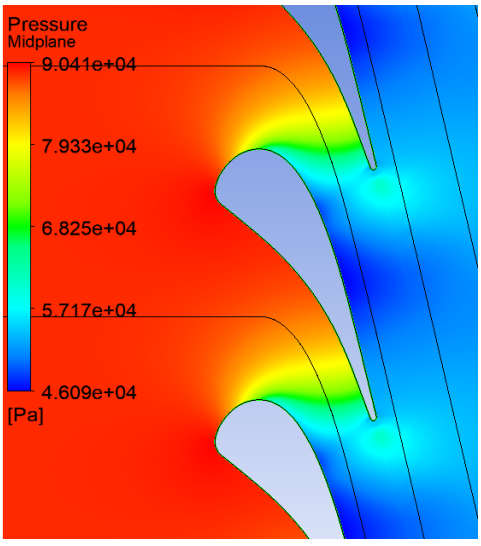

Figure 38: Static pressure [configuration : line 5 of the table 1]

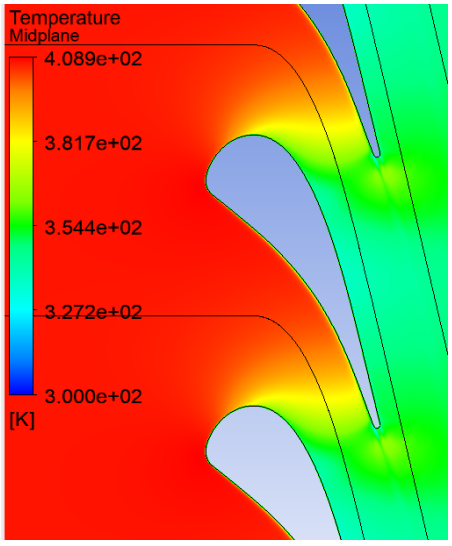

Figure 39: Temperature [configuration : line 5 of the table 1]

and the coarse grid for the SST simulation. The effect of numerical diffusion was small and had biggest effect on the fine grid as expected. The effect of changing turbulence model was almost negligible. Since the results for all the cases are so consistent it suggests some reliability. At the same time, the same sources of error may have manifested in the five cases, and the results can not be completely validated by comparing the conducted simulations alone. For example, the choice of outlet may have created a bias for all the simulation. Another thing to consider is that the amount of cells in the fine grid should have been higher in order to see the different effects clearer. But as mentioned in the section 4.1 much of the results are as expected from the behaviour of an airfoil. Also the results presented in this report are similar to those presented by F. Kiyici et al. [1] for a similar configuration. Hence, that confirms the reliability of our results.

The grid refinement should be adapt according to the problem set. A fine grid provide grid-independent solutions that can be analyzed further but that may not be necessary. The choice of the time scheme have to be defined according to the refinement of the grid and the precision of values required for the study that wants to be done. For a coarse grid a low order method would be preferable to an high one and vice versa. In this study grid refinement have less influence on the solution than the choice of the time scheme. That an other parameter to take into account to reduce time computing in the most efficient way. The choice of the turbulence model needs to be based on the physic aspect of the study. Elements that can be neglected and other that have to be considered have to be known to make sure that the turbulence model used would fit with it.

In some cases, for instance in industry in the early stages of the conception of a design or in research in the preliminary studies, a coarser grid with a low order time scheme should be enough to provide the clues to know what are the next simulation to make. If the results in the conducted simulation is not too invalid, a lower order upwind scheme on a coarser grid can provide sufficient accuracy maybe except for the lift force. CFD configuration for simulation must always be based on the problem studied and on the desired precision for the results.

References

[1] Firat Kiyici, Tolga Yasa, Emiliano Costa, and Porziani Stefano. Cfd optimization of transonic low pressure turbine blade. *Ninth International Conference on Computational Fluid Dynamics*, 2016.

[2] F. R. Menter, A. V. Garbaruk, and Y. Egorov. Explicit algebraic reynolds stress models for anisotropic wall-bounded flows. *EUCASS – 3rd European Conference for Aero-Space Sciences*, 2009.

[3] William Sutherland. Lii. the viscosity of gases and molecular force. *The London, Edinburgh, and Dublin Philosophical Magazine and Journal of Science Serie 5*, 36(223):507–531, 1893.

[4] Bram van Leer. Upwind and high-resolution methods for compressible flow : From doner cell to residual-distribution schemes. *Communications in computational physics*, 1(2):192–206, 2006.